

High- quality factor poly (vinylidene fluoride) based novel nanocomposites filled with graphene nanoplatelets and vanadium pentoxide for high-Q capacitor applications

Kumar Digvijay Satapathy¹, Kalim Deshmukh¹, M. Basheer Ahamed^{1*}, Kishor Kumar Sadasivuni², Deepalekshmi Ponnamm³, S. K. Khadheer Pasha⁴, Mariam Al-Ali AlMaadeed³, Jamil Ahmad⁵

¹Department of Physics, B.S. AbdurRahman University, Chennai 600048, TN, India

²Mechanical & Industrial Engineering Department, Qatar University, P.O. Box 2713, Doha, Qatar

³Center for Advanced Materials, Qatar University, P.O. Box 2713, Doha, Qatar

⁴Department of Physics, School of Advanced Sciences, VIT University, Vellore-632014, TN, India

⁵Department of Chemical Engineering, University of Engineering and Technology, Peshawar, Pakistan

*Corresponding author, Tel :(+91) 9500101398; E-mail: mbasheerahamed133@gmail.com

Received: 16 March 2016, Revised: 21 June 2016 and Accepted: 22 November 2016

DOI: 10.5185/amlett.2017.6539

www.vbripress.com/aml

Abstract

Herein, we report the synthesis of poly (vinylidene fluoride) (PVDF) based novel nanocomposites reinforced with graphene nanoplatelets (GNP) and vanadium pentoxide (V_2O_5) as nanofillers. The PVDF/ V_2O_5 /GNP nanocomposite films were characterized using Fourier transform infrared spectroscopy (FTIR), X-ray diffraction analysis (XRD), thermogravimetric analysis (TGA), polarized optical microscopy (POM) and scanning electron microscopy (SEM). The electrical properties of nanocomposites were investigated to ascertain the synergistic effect of fillers on the quality factor (Q-factor) of nanocomposites. The FTIR and XRD results infer good interaction between PVDF and V_2O_5 and the good dispersion of nanofillers in the PVDF matrix. The TGA results revealed that the thermal stability of PVDF/ V_2O_5 /GNP nanocomposite has improved at higher loading of nanofillers due to the good interaction between the nanofillers and the polymer matrix. The electrical analysis of nanocomposite films demonstrates high Q-factor value (1099.04) at 4.7 wt % V_2O_5 and 0.3 wt % GNP loading. With further increase in GNP loading to 1 wt %, the Q-factor becomes lower (356.52) which could be due to the enhanced conductivity of the samples. The significant enhancement in the value of Q-factor shows that the nanocomposites can be used as a potential candidate for high-Q capacitor applications. Copyright © 2017 VBRI Press.

Keywords: Graphene nanoplatelets, PVDF, V_2O_5 , high-Q capacitors.

Introduction

With day to day improvisation in this so called technological society, the requirements of the new materials having special properties like high-quality factor (Q-factor) is useful for various applications such as medical devices, consumer products, food packaging, aerospace technologies for sensing and also for coating and barrier applications. The materials having a high Q-factor play a remarkable role in designing microelectronic devices and to analyze microscopic processes. Polymers are the most widely used materials because of their low cost, reproducibility and easy processing [1-5]. Poly (vinylidene fluoride) (PVDF) is one of the most studied polymeric systems because of its excellent piezoelectric and pyroelectric properties [6]. PVDF attracts the attention of engineers and physicists as a stimuli-responsive polymer having four crystal polymorphs such as α , β , γ and δ [7, 8]. β - phase of PVDF has shown great

potential as a polymeric matrix for functional applications because of its good physical and chemical properties, good processability and favorable electrical, thermal and mechanical properties [9].

Since the discovery of graphene by Geim, Novoselov and co-workers in 2004 [10, 11], it has evolved as one of the ideal carbon-based nanomaterials. Graphene belongs to the family of graphitic materials with a two-dimensional (2-D) structure, arranged in a honeycomb crystal lattice of sp^2 bonded carbon atoms [12]. Graphene can be obtained easily from abundant natural or synthetic resources without enormous energy consumption [13]. Graphene has been used extensively by the researchers all over the world due its extraordinary optical, mechanical and physical properties such as high surface area (2630 m^2/g), Young's modulus (1TPa), fracture strength (130 GPa) and thermal (5 Wm^{-1}) and electrical conductivity of (720 Sm^{-1}) [14, 15]. Graphene has the ability to be dispersed in polymer matrices and it has gained both

academic and industrial interest as it can produce a dramatic improvement in properties of the polymer matrix with a small amount of loading [16]. Polymer nanocomposites based on graphene nanoplatelets (GNP) evolved as a new class of materials having extraordinary potential for many applications. Graphene-based nanocomposites have fascinating applications such as field effect transistors [17], high-performance composites [18] and lithium ion batteries [19]. The graphene oriented applications have motivated scientists and engineers all over the world in producing novel graphene-based polymer nanocomposites. The host polymers show significant improvement in its physical properties by improving the exfoliation and dispersion of graphene and by producing stronger interactions with the polymer matrix through the proper interaction of functional groups on the surface of graphene.

Various metal oxides such as MnO_2 , V_2O_5 , SiO_2 , and TiO_2 demonstrated their technological applications as catalytic material [19], in electrochromic devices [20], as battery cathode material [21], and sensors [22, 23]. Out of these oxides, V_2O_5 shows notable physical and chemical properties. The multiple valence states and its rich structural chemistry make its molecule (or ion) [24] capable of inserting into the compounds. This lamellar layered material is one of the most stable oxides in V-O systems and possesses great potential to change its optical and electrical properties. However, only a few experimental studies have been performed on polymer/ V_2O_5 composites. The metal-semiconductor transition nature of V_2O_5 could be helpful in increasing the Q-factor of the polymer matrix. Taking this into account, V_2O_5 has been used as the second filler in the present study.

Here, the PVDF/ V_2O_5 /GNP nanocomposite films were prepared and characterized using FTIR, XRD, TGA, optical microscopy and SEM analyses. The Q-factor of nanocomposite films was obtained as a function of frequency at four different temperatures in order to check their feasibility for high-Q capacitor applications.

Experimental

Materials

Poly (vinylidene fluoride) powder was purchased from Pragati Plastics Pvt. Ltd., India. The V_2O_5 powder was supplied by Yogi Dye Chem Industries, Ghatkopar, Mumbai, India. Graphene nanoplatelets (Type 1) with surface area, $150 \text{ m}^2/\text{g}$, thickness ranging from 6-8 nm and average particle size (APS) 15 micron was purchased from Sisco Research Laboratories Pvt. Ltd, Chennai, India. Dimethylformamide (DMF) was purchased from S. D. Fine Chemicals, Mumbai, India.

Preparation of PVDF/ V_2O_5 /GNP nanocomposite films

PVDF/ V_2O_5 /GNP nanocomposite films were prepared by colloidal blending method as per the procedure described in Fig. 1. The desired amount of PVDF powder was first dissolved in DMF at 70°C for 2 h in a hot air oven. Later, GNP and V_2O_5 were dispersed separately in DMF and sonicated for 1 hr. The resulting homogeneous dispersions

of GNP and V_2O_5 were then added to the PVDF solution and stirred vigorously for 6 h. After that, the PVDF/ V_2O_5 /GNP colloidal mixture was spread onto a Teflon Petri dish and dried in the hot air oven at 70°C for 4 h.

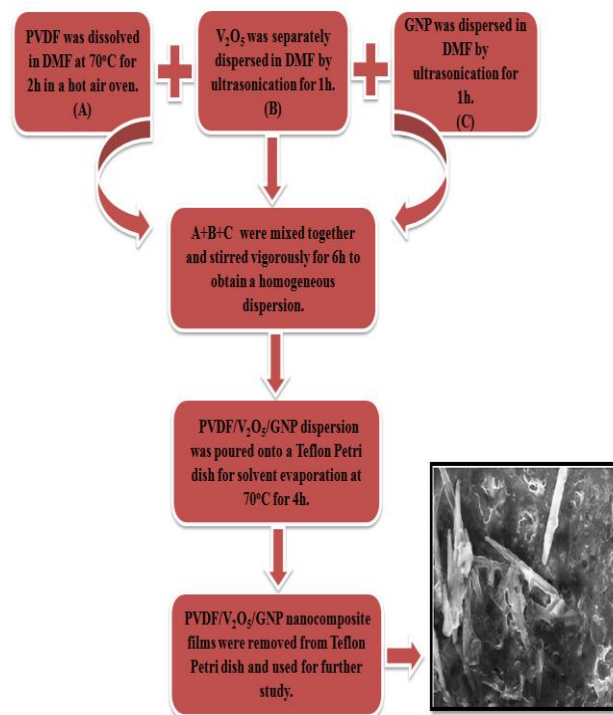


Fig. 1. Protocol for the synthesis of PVDF/ V_2O_5 /GNP nanocomposite films.

After solvent evaporation, the PVDF/ V_2O_5 /GNP nanocomposite films were obtained. The percentage loading of the GNP and V_2O_5 in PVDF/ V_2O_5 /GNP nanocomposite were varied from 0.3 to 1 wt% and 5 to 4 wt% respectively, as shown in Table 1.

Table 1. Feed composition of PVDF/ V_2O_5 /GNP nanocomposite films.

No.	PVDF (wt %)	V_2O_5 (wt %)	GNP (wt %)
1	100	0	0
2	95	5	0
3	95	4.7	0.3
4	95	4.5	0.5
5	95	4.3	0.7
6	95	4	1

Characterizations

FTIR spectroscopy of GNP, V_2O_5 , PVDF, PVDF/ V_2O_5 and PVDF/ V_2O_5 /GNP nanocomposite films was carried out in a transmittance mode using FTIR spectrophotometer (JASCO -6300) in the wave number range from $400\text{--}4000 \text{ cm}^{-1}$ with a spectral resolution of 4 cm^{-1} .

The X-ray diffraction of PVDF, GNP, V_2O_5 , PVDF/ V_2O_5 and PVDF/ V_2O_5 /GNP nanocomposite films with different compositions were studied using an advanced X-ray diffractometer (D8 Bruker, Germany). The scans were taken in the 2θ range from $10\text{--}90^\circ$ using Cu K α radiation of wavelength $\lambda = 1.54060 \text{ \AA}$.

The dispersion state of PVDF/V₂O₅ and PVDF/V₂O₅/GNP nanocomposites were studied using optical microscopy (Axio Scope A1, Carl Zeiss, Germany) at a magnification of 10X. The microstructure and surface morphology of GNP, V₂O₅ and PVDF/V₂O₅/GNP nanocomposite films were analyzed by scanning electron microscope (SU6600, HI-2108-0002, Japan) equipped with a secondary electron detector. The analysis was conducted at various pressure modes. The samples were gold coated and an accelerating voltage of 15 kV was applied to obtain the SEM micrographs. SEM micrographs at X 5,000 magnification were taken. Thermal stability of GNP, V₂O₅ and PVDF/V₂O₅/GNP nanocomposite films were evaluated using thermogravimetric analyzer (TG/DTA 6200, SII Nano Technology, Japan). The samples were heated up to 600°C under N₂ atmosphere at the heating rate of 20°C/min.

The current-voltage characteristics of pure PVDF and PVDF/V₂O₅/GNP nanocomposite films were studied by using the two probes Keithley source meter at room temperature and relative humidity 30%. The voltage was changed from 0 to +40 V using a scientific power supply for each step of 30s, in the forward bias.

The Q-factor measurements were carried out by using an impedance analyzer (Hioki 3532-50 LCR Hitester, UK). The samples were tested as a function of frequency ranging from 50 Hz to 5 MHz and at four different temperatures.

Results and discussion

FTIR spectroscopy

The FTIR spectroscopy was performed to identify the reactive functional groups and to study the interactions among the atoms and ions of PVDF, V₂O₅ and GNP. The FTIR spectra of GNP, V₂O₅ and PVDF are shown in Fig. 2. There is no remarkable peak in the FTIR spectrum of GNP (Fig. 2(a)), which is mainly because of the absence of oxygen species in the graphene. Fig. 2(b) shows FTIR spectrum of pure V₂O₅, in which a low-frequency band was observed at 516 cm⁻¹ which can be attributed to symmetric stretching vibrations of the V-O-V group.

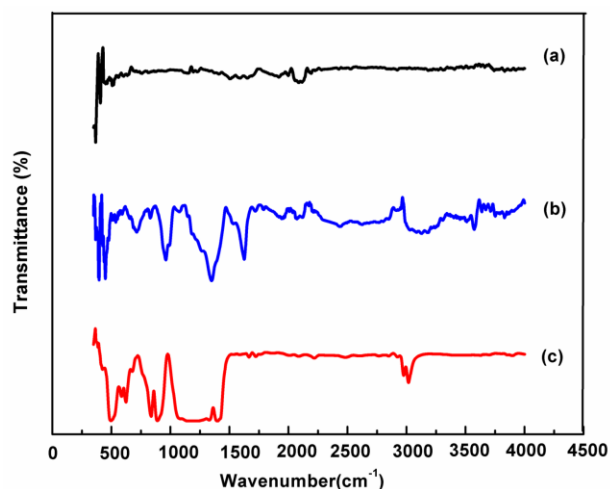


Fig. 2. FTIR spectra of (a) GNP (b) V₂O₅ (c) PVDF.

The bands at 726 and 837 cm⁻¹ were also observed in FTIR spectrum of pure V₂O₅ which is attributed to asymmetric stretching vibrations of the V-O-V group. The band obtained at 993 cm⁻¹ is attributed to the presence of V=O stretching vibrations. The band appearing at 3499 and 3576 cm⁻¹ are due to O-H stretching vibration [25]. From Fig. 2(c), it can be seen that the FTIR spectrum of PVDF shows the characteristic absorption bands at 598 and 846 cm⁻¹ attributed to respective CF₂ bending and CH₂ rocking. The FTIR bands at 3019 and 2977 cm⁻¹ are respectively due to the asymmetric and symmetric stretching vibration of the CH₂ group [26]. The FTIR spectra of PVDF/V₂O₅ (95/05) and PVDF/V₂O₅/GNP nanocomposites with different V₂O₅ and GNP loadings are shown in Fig. 3. The FTIR spectra of PVDF/V₂O₅/GNP nanocomposite films show various FTIR peaks which are common in the FTIR of individual components. The bands of asymmetric (3019 cm⁻¹) and symmetric (2977 cm⁻¹) stretching vibration of CH₂ groups of PVDF were shifted to (2977 cm⁻¹ and 3011 cm⁻¹) for PVDF/V₂O₅ composites; (2978 cm⁻¹ and 3019 cm⁻¹) for nanocomposites with 0.3 wt % GNP and 4.7 wt % V₂O₅, (2985 cm⁻¹ and 3012 cm⁻¹) for 0.5 wt % GNP and 4.5 wt % V₂O₅, (2976 cm⁻¹ and 3012 cm⁻¹) for 0.7 wt % GNP and 4.3 wt % V₂O₅, (2979 cm⁻¹ and 3014 cm⁻¹) for 1 wt % GNP and 4 wt % V₂O₅. Also, the peaks around 3576 cm⁻¹ appeared due to the presence of moisture in V₂O₅. Thus, from the FTIR study, it can be seen that there is a good interaction between PVDF and V₂O₅ and a good dispersion of GNP and V₂O₅ in the PVDF matrix.

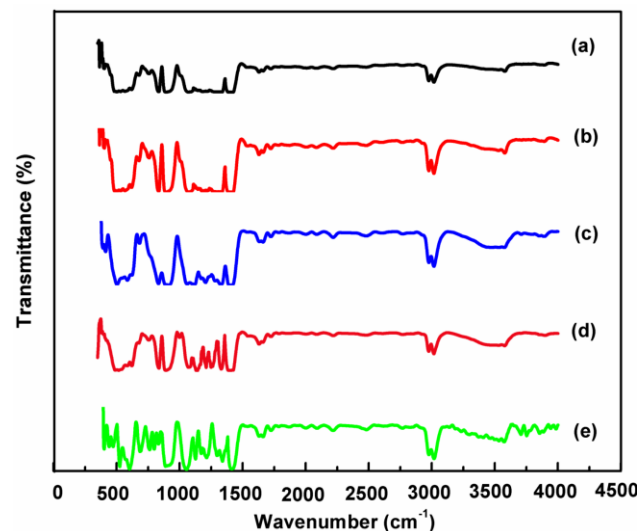


Fig. 3. FTIR spectra of PVDF/V₂O₅/GNP nanocomposite films (a) PVDF/V₂O₅ (b) 0.3 wt% GNP (c) 0.5 wt% GNP (d) 0.7 wt% GNP (e) 1 wt% GNP.

X-ray diffraction studies

X-ray diffraction is an effective method to investigate the crystalline properties of synthesized nanocomposites. The XRD patterns of neat PVDF, V₂O₅, GNP and PVDF/V₂O₅/GNP nanocomposites are illustrated in Fig. 4(a) and Fig. 4b (i-vii). The XRD pattern of PVDF powder (Fig. 4(a)) shows a broad peak at 19.26° which correspond to α -phase of PVDF [27]. The XRD pattern of

PVDF also showed two more characteristic peaks at $2\theta = 35^\circ$ and 40.3° . The XRD pattern of GNP showed a broad reflection peak at $2\theta = 26.2^\circ$ (**Fig. 4b (i)**) with an interlayer spacing of 0.36 nm, indicating the crystalline nature of GNP [28, 29]. In **Fig. 4b (ii)**, the XRD pattern of pure V_2O_5 shows different characteristics diffraction peaks at $2\theta = 25.84^\circ$ (110), $2\theta = 30.2^\circ$ (400), $2\theta = 32.3^\circ$ (011) and $2\theta = 39.12^\circ$ (002). The XRD pattern of the pure V_2O_5 indicates that the V_2O_5 used in the present study belongs to the orthorhombic crystal symmetry [JCPDS-41-1426]. The XRD pattern of PVDF/ V_2O_5 (95/5) and PVDF/ V_2O_5 /GNP nanocomposite films shows a single diffraction peak at $2\theta = 19.76^\circ$ (**Fig 4b (iii-vii)**) which is associated with the crystalline peak of PVDF. The XRD peaks corresponding to GNP and V_2O_5 were not seen in the XRD pattern of PVDF/ V_2O_5 /GNP nanocomposites which could be due to the structural disorder in the nanocomposite films [30, 31].

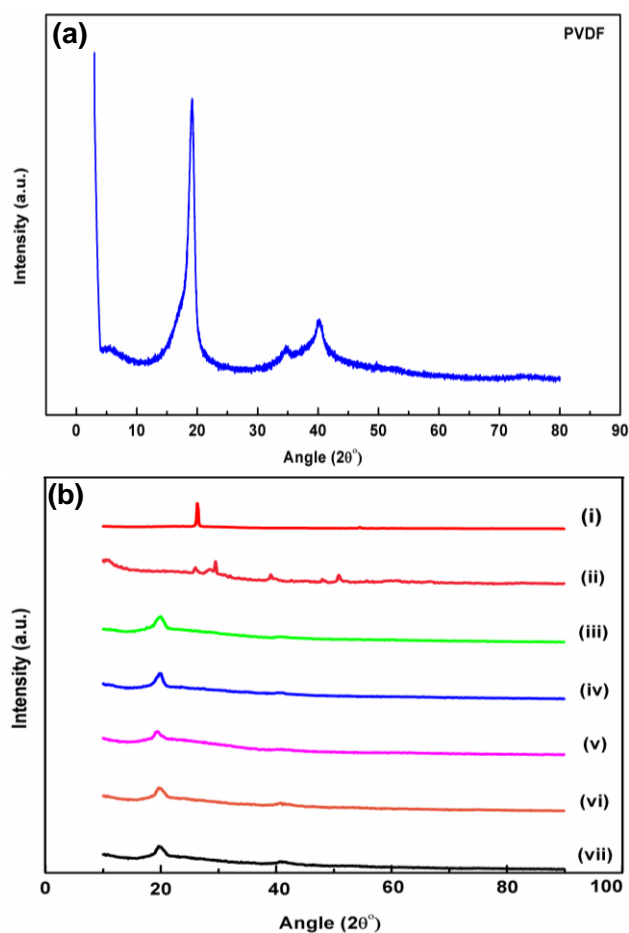


Fig. 4. (a). XRD pattern of PVDF powder (b). XRD pattern of PVDF/ V_2O_5 /GNP nanocomposite films (i) GNP (ii) V_2O_5 powder (iii) PVDF/ V_2O_5 (iv) 0.3 wt% GNP (v) 0.5 wt% GNP (vi) 0.7 wt% GNP (vii) 1 wt% GNP.

Morphology and microstructure

Optical microscopy is one of the most useful techniques to identify the dispersion state of nanofillers and it helps in understanding the reinforcement effect of fillers in the polymer matrix. It also provides information about the morphology and degree of agglomeration ranging from several micrometers to millimeters. Optical microscopy of

PVDF/ V_2O_5 /GNP nanocomposite films was studied to understand the reinforcement effect of V_2O_5 and GNP in PVDF matrix. **Fig. 5** shows optical microscopy images of PVDF/ V_2O_5 /GNP nanocomposites. It can be observed that GNP and V_2O_5 have been dispersed homogeneously throughout the PVDF matrix without any obvious agglomerations. The microstructure of nanocomposites was further examined by SEM analysis.

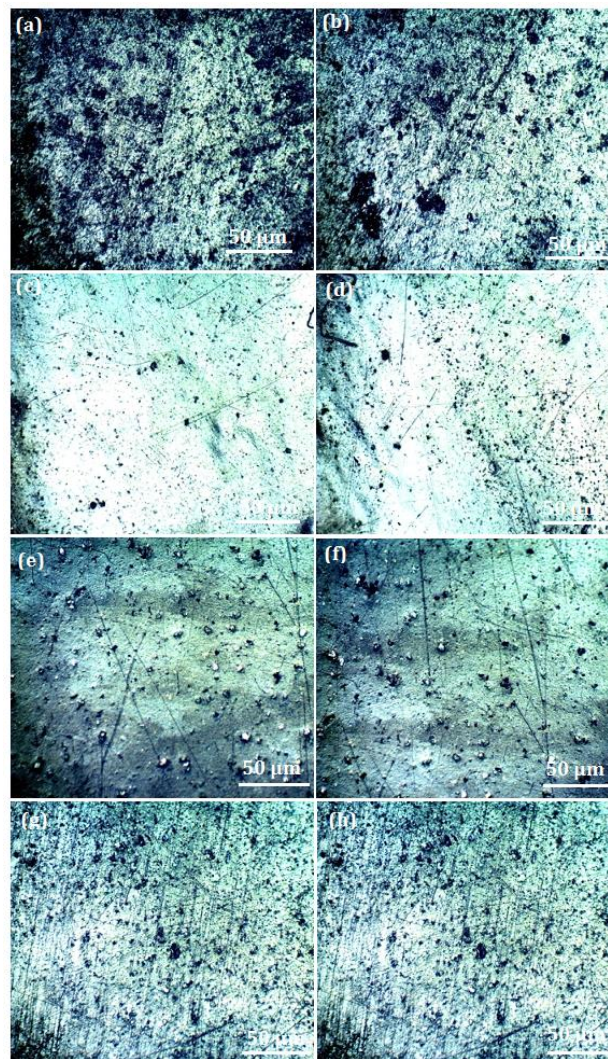


Fig. 5. Optical microscopy images of PVDF/ V_2O_5 /GNP nanocomposite films (a,b) 0.3 wt % GNP (c,d) 0.5 wt % GNP (e,f) 0.7 wt % GNP (g,h) 1 wt% GNP.

SEM is a powerful technique to study the interfacial interactions between the constituents of polymer nanocomposites. The SEM micrographs of GNP, V_2O_5 and PVDF/ V_2O_5 /GNP nanocomposites are depicted in **Fig 6(a-f)**. The SEM micrographs of GNP as shown in **Fig. 6(a, b)**, indicates a wrinkled surface morphology which is a highly favorable medium for strong interfacial interaction with polar polymers. From the SEM micrographs of V_2O_5 shown in **Fig. 6(c, d)**, a porous network of nanobelts can be seen. The SEM micrographs of PVDF/ V_2O_5 /GNP nanocomposite film with 0.7 wt% of GNP is shown in **Fig. 6(e, f)**. SEM micrographs demonstrate that the majority of GNP and V_2O_5 have been uniformly dispersed throughout the polymer matrix and

individual phases of PVDF, GNP and V_2O_5 were difficult to distinguish. This type of morphology of the nanocomposites leads to higher capacitance and cycling life during the charge-discharge process of capacitors [29-32].

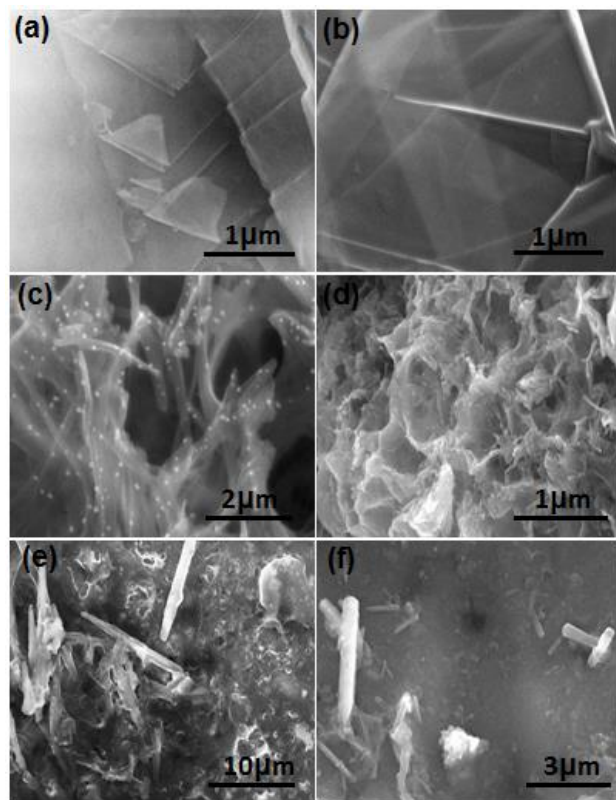


Fig. 6. SEM micrographs of (a, b) GNP (c, d) V_2O_5 powder (e, f) PVDF/ V_2O_5 /GNP nanocomposite film with 0.7 wt % GNP loading.

Thermogravimetric analysis (TGA)

The thermal stability is an important property of polymer nanocomposites for their application point of view. The incorporation of nanofillers can significantly enhance the thermal stability of the polymer matrix. To demonstrate this possibility, PVDF/ V_2O_5 /GNP nanocomposite films were studied by TGA. The weight loss of all the samples due to degradation is monitored as a function of temperature. The TGA curves of GNP, V_2O_5 and PVDF/ V_2O_5 /GNP nanocomposites are depicted in **Fig. 7**. The TGA curve of pure GNP powder is shown in **Fig. 7(a)**. It can be observed that from 100 to 600°C GNP shows only 18% weight loss, indicating its excellent thermal stability. On the other hand, the TGA curve of V_2O_5 powder (**Fig. 7(b)**) shows two major decomposition steps. First weight loss is just above 100°C which could be due to the loss of absorbed water. The second weight loss is in the temperature range of 380-400°C can be attributed to the removal of residual water from vanadyl group. Pure V_2O_5 showed 32 % weight loss when heated up to 600°C. Thus, it can be noted that the GNP is thermally more stable than V_2O_5 . The TGA curve of pure PVDF powder is shown in **Fig. 7(c)**. It can be seen that pure PVDF showed negligible weight loss (only 1%) up to 340°C. With further increase in temperature, the weight loss increases sharply and complete decomposition

occurred. This indicates that PVDF is thermally stable up to 340°C. The TGA curves of PVDF/ V_2O_5 /GNP nanocomposites films are depicted in **Fig 7 (d-g)**. The PVDF/ V_2O_5 /GNP nanocomposites containing 0.3 and 0.5 wt% GNP loadings show two-stage decomposition behavior. However, the decomposition temperature is around 330°C (17.5 % weight loss) for nanocomposites containing 0.3 wt % GNP loading and 325°C (18 % weight loss) for nanocomposites containing 0.5 wt % GNP loading. In addition, from the TGA curves of PVDF/ V_2O_5 /GNP nanocomposites containing 0.7 and 1 wt% GNP loading, it can be seen that the decomposition temperature is shifted towards higher temperature as compared to the nanocomposites containing 0.3 and 0.5 wt % GNP loading. The % weight loss for nanocomposites containing 0.7 wt % GNP was found to be 17% at 430°C and that of 1 wt % GNP loading was found to be 20% at 460°C. This indicates that the thermal stability of nanocomposites containing 0.7 and 1 wt % GNP is better than the nanocomposites containing 0.3 and 0.5 wt % GNP. Thus, TGA results indicate enhanced thermal stability of nanocomposites at higher loadings of GNP.

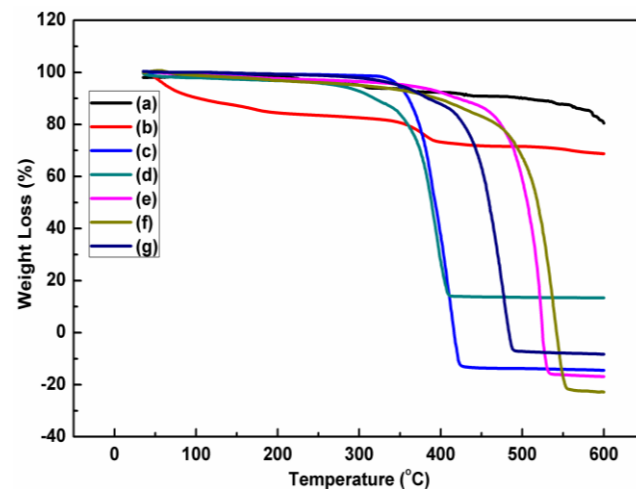


Fig. 7. TGA thermograms of PVDF/ V_2O_5 /GNP nanocomposites (a) GNP (b) V_2O_5 (c) PVDF (d) 0.3 wt% GNP (e) 0.5 wt% GNP (f) 0.7 wt% GNP (g) 1 wt% GNP.

Electrical Properties

The current-voltage characteristic is very useful in determining the operating conditions of a particular electronic device or component and shows the possible combinations of current and voltage. The current-voltage relationship of pure PVDF and PVDF/ V_2O_5 /GNP nanocomposite films with different V_2O_5 and GNP loading is shown in **Fig. 8**. It can be seen that the potential difference (in volt) increases linearly with applied current (mA), which confirms the semiconductor behavior of nanocomposites. With an increase in the GNP loading in the polymer matrix, the conducting nature of the PVDF/ V_2O_5 /GNP nanocomposites increases gradually with respect to the applied current. Furthermore, the Q-factor of nanocomposites was also investigated to check their feasibility for high-Q capacitor applications. The Q-factor is a dimensionless parameter, which defines

how the system (oscillator or resonator) oscillates with the amplitude which gradually decreases to zero.

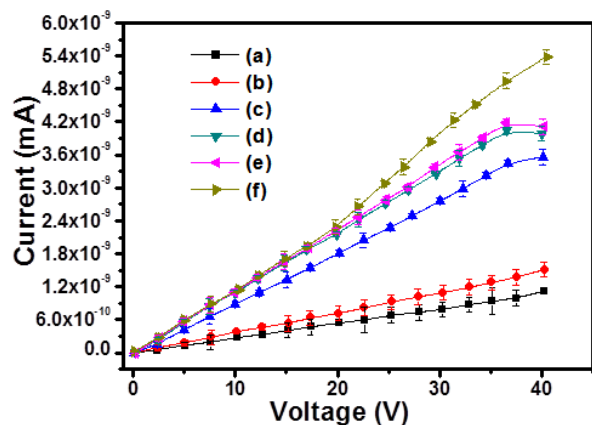


Fig. 8. I-V curves of PVDF and PVDF/V₂O₅/GNP nanocomposites (a) PVDF (b) 5 wt% V₂O₅ (c) 0.3 wt% GNP (d) 0.5 wt% GNP (e) 0.7 wt% GNP (f) 1 wt% GNP.

Q-factor plays an important role in the characterization of the resonant tank circuit or LC circuit. Q-factor can be defined as

$$Q = 2\pi \frac{\text{Maximum energy stored per cycle}}{\text{Maximum energy dissipated per cycle}}$$

Q-factor can also be considered as a ratio of the required quantity related to the inductive reactance to the unwanted quantity i.e. resistance.

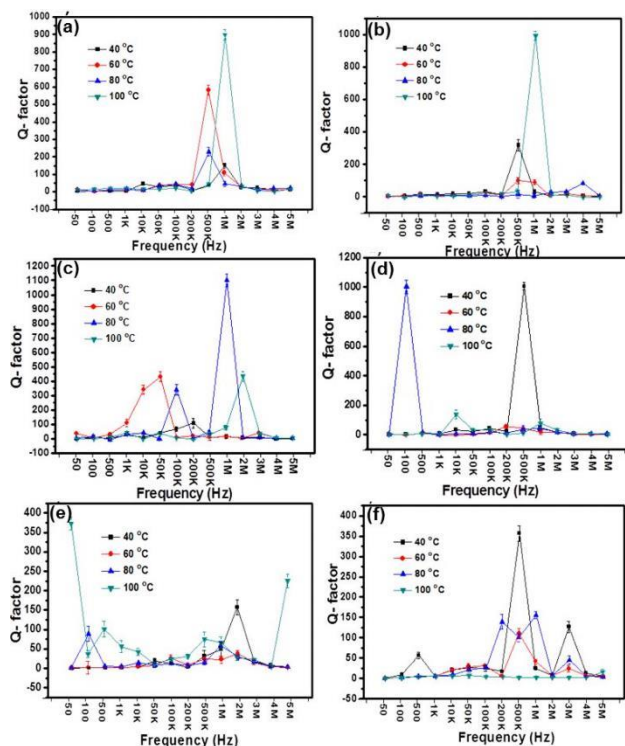


Fig. 9. Q-factor of (a) PVDF film (b) PVDF/V₂O₅ (95/05) nanocomposite (c) PVDF/V₂O₅/GNP nanocomposite with 0.3 wt% GNP loading (d) Q - factor of PVDF/V₂O₅/GNP nanocomposite with 0.5 wt% GNP loading (e) PVDF/V₂O₅/GNP nanocomposite with 0.7 wt% GNP loading (f) PVDF/V₂O₅/GNP nanocomposite with 1 wt% GNP as a function of frequency at four different temperatures.

In this investigation, the incorporation of GNP into the PVDF matrix increases the Q-factor at high frequencies via the high-frequency characteristics (> 1 MHz). The values of Q-factor for PVDF/V₂O₅/GNP nanocomposites were shown in **Fig. 9(a-f)** as a function of frequency and temperature. It can be seen that the Q-factor for nanocomposites containing 5 wt% V₂O₅ and 4.7 wt% GNP is 997.97 and 1099.04 respectively evidencing that GNP offers a high degree of electromagnetic interference (EMI) response. However, from the **Fig. 9 (d-f)**, it can be observed that the Q-factor decreases gradually in the PVDF/V₂O₅/GNP nanocomposite films with further increase in the GNP loading. The inductance values also decrease by increasing GNP loading which indicates an increase in the conductivity. So the Q-factor and the conductivity are inversely proportional to each other. The Q-factor and inductance values obtained for PVDF/V₂O₅/GNP nanocomposites are given in **Table 2**. Also, it can be seen that GNP loading increases conductivity, whereas the increase in wt % of V₂O₅ increases the Q-factor value of the PVDF/V₂O₅/GNP nanocomposite films. The results obtained from the electrical analysis confirm that PVDF/V₂O₅/GNP nanocomposite can be used as a potential candidate for high Q-capacitor applications.

Table 2. Q - factor and inductance values of PVDF/V₂O₅ and PVDF/V₂O₅/GNP nanocomposite films.

Sample Name	Q - factor (Q)	Inductance (G)
PVDF	889.99, 1MHz, 100°C	1.216×10 ⁻⁴ , 5MHz, 100°C
PVDF/V ₂ O ₅	997.97, 1MHz, 80°C	3.935×10 ⁻⁴ , 5MHz, 100°C
0.3 wt% GNP loading	1099.04, 1MHz, 80°C	1.316×10 ⁻⁴ , 5MHz, 100°C
0.5 wt% GNP loading	989.99, 100Hz, 80°C	9.892×10 ⁻⁵ , 3MHz, 100°C
0.7 wt% GNP loading	370.91, 50Hz, 100°C	9.555×10 ⁻⁵ , 3MHz, 100°C
1 wt% GNP loading	356.52, 500Hz, 40°C	2.204×10 ⁻⁵ , 5MHz, 100°C

Conclusion

In summary, PVDF/V₂O₅/GNP novel nanocomposite films were successfully prepared by colloidal blending and their characteristics were examined using different analytical techniques, such as FTIR, TGA, XRD, polarized optical microscopy and SEM. FTIR and XRD results infer a good interaction between PVDF and V₂O₅ and a good dispersion of GNP and V₂O₅ in the PVDF matrix. SEM micrographs of PVDF/V₂O₅/GNP nanocomposite films reveal that V₂O₅ and GNP were uniformly dispersed within the polymer matrix. The investigation of thermal properties by means of TGA revealed that the GNP have better thermal stability than V₂O₅ and the thermal stability of PVDF/V₂O₅/GNP nanocomposite has improved at higher loading of nanofillers due to the good interaction between the nanofillers and the polymer matrix. The results of the current-voltage characteristics indicate the semiconductor behavior of PVDF/V₂O₅/GNP nanocomposites.

Furthermore, with an increase in the GNP loading, the conducting behavior of the PVDF/V₂O₅/GNP nanocomposites increases gradually with respect to the applied current. From the electrical properties of nanocomposites, it can be noted that the addition of V₂O₅ enhances the Q-factor of PVDF/V₂O₅/GNP nanocomposite films. The low loading of GNP shows a significantly high Q-factor value indicating the low energy loss in the nanocomposites. The nanocomposites with 4.7 wt% V₂O₅ and 0.3 wt % GNP loading showed Q-factor value of about 1099.04. With further increase in GNP loading to 1 wt %, the Q-factor has decreased to 356.52, which could be due to the enhanced conductivity of the samples. Thus, the results from the electrical properties of PVDF/V₂O₅/GNP nanocomposites demonstrate that these novel nanocomposites with high Q-factor can be used as a potential candidate for high Q - capacitor applications.

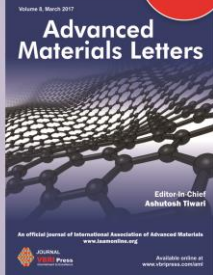
Acknowledgement

The authors would like to acknowledge the instrumental facility provided by the Qatar University, Doha, Qatar during this research work.

References

- Pawde, S.M.; Deshmukh, K.; *J. Appl Polym. Sci.*, **2009**, 114, 2169.
DOI: [10.1002/app.30641](https://doi.org/10.1002/app.30641)
- Ahmad, J.; Deshmukh, K.; Hägg, M.B.; *Int. J. Polym. Anal. Charact.*, **2013**, 18, 287.
DOI: [10.1080/1023666X.2013.767080](https://doi.org/10.1080/1023666X.2013.767080)
- Deshmukh, K.; Ahamed, M.B.; Deshmukh, R.R.; Bhagat, P.R.; Pasha, S.K.K.; Bhagat, A.; Shirbhate, R.; Telare, F.; Lakhani, C.; *Polym. Plast. Tech. Eng.*, **2016**, 55, 231.
DOI: [10.1080/03602559.2015.1055499](https://doi.org/10.1080/03602559.2015.1055499)
- Pasha, S.K.K.; Deshmukh, K.; Ahamed, M.B.; Chidambaram, K.; Mohanapriya, M.K.; Nambi Raj, N.A.; *Adv. Polym. Tech.*, **2015**.
DOI: [10.1002/adv.21616](https://doi.org/10.1002/adv.21616)
- Ahmad, J.; Deshmukh, K.; Habib, M.; Hägg, M.B.; *Arab. J. Sci. Eng.*, **2014**, 39, 6805.
DOI: [10.1007/s13369-014-1287-0](https://doi.org/10.1007/s13369-014-1287-0)
- Kim, H.; Baik, D.H.; Jeong, Y.G.; *Macromol. Res.*, **2012**, 20, 920.
DOI: [10.1007/s13233-012-0064-8](https://doi.org/10.1007/s13233-012-0064-8)
- Salimi, A.; Yousefi, A.A.; *Polym. Test.*, **2003**, 22, 699.
DOI: [10.1016/S0142-9418\(03\)00003-5](https://doi.org/10.1016/S0142-9418(03)00003-5)
- Jing, X.; Shen, X.; Song, H.; Song, F.; *J Polym Res*, **2011**, 18, 2017.
DOI: [10.1007/s10965-011-9610-x](https://doi.org/10.1007/s10965-011-9610-x)
- Pawde, S.M.; Deshmukh, K.; *Polym. Eng. & Sci.*, **2009**, 49, 808.
DOI: [10.1002/pen.21319](https://doi.org/10.1002/pen.21319)
- Mensah, B.; Kumar, D.; Lim, D.K.; Kim, S.G.; Jeong, B.H.; Nah, C.; *J. Appl Polym Sci.*, **2015**, 4, 132.
DOI: [10.1002/app.42457](https://doi.org/10.1002/app.42457)
- Geim, A.K.; *Science*, **2009**, 324, 1530.
DOI: [10.1126/science.1158877](https://doi.org/10.1126/science.1158877)
- Parlak, O.; Turner, A.P.F.; Tiwari, A.; *Advanced Materials*, **2014**, 26, 482.
DOI: [10.1002/adma.201303075](https://doi.org/10.1002/adma.201303075)
- Tiwari, A.; (Eds), In the Graphene materials: Fundamentals and emerging applications, John Wiley & Sons, USA, **2015**.
- Lee, C.; Wei, X.; Kysar, J.W.; Hone, j.; *Science*, **2008**, 321, 385.
DOI: [10.1126/science.1157996](https://doi.org/10.1126/science.1157996)
- Deshmukh, K.; Ahamed, M.B.; Deshmukh, R.R.; Pasha, S.K.K.; Sadasivuni, K.K.; Ponnammam, D.; Chidambaram, K.; *Euro. Polym. J.*, **2016**, 76, 14.
DOI: [10.1016/j.eurpolymj.2016.01.022](https://doi.org/10.1016/j.eurpolymj.2016.01.022)
- Das, T.K.; Prusty, S.; *Polym. Plast. Tech. Eng.*, **2013**, 52, 319.
DOI: [10.1080/03602559.2012.751410](https://doi.org/10.1080/03602559.2012.751410)
- Sharon, M.; Sharon, M.; Shinohara, H.; Tiwari, A.; (Eds), In the Graphene: An Introduction to the Fundamentals and Industrial Applications, Wiley, USA, **2015**.
- Kim, H.; Abdala, A.A.; Macosko, C.W.; *Macromolecules*, **2010**, 43, 6515.

- DOI: [10.1021/ma100572e](https://doi.org/10.1021/ma100572e)
- Wang, H.; Cui, L.-F.; Yang, Y.; Casalongue, S.H.; Robinson, J.T.; Liang, Y.; Cui, Y.; Dai, H.; *J. Am. Chem. Soc.* **2010**, 132, 13978.
DOI: [10.1021/ja105296a](https://doi.org/10.1021/ja105296a)
 - Karunakaran, C.; Senthilvelan, S.; *J. Colloid Interface Sci.*, **2005**, 289, 466.
DOI: [10.1016/j.jcis.2005.03.071](https://doi.org/10.1016/j.jcis.2005.03.071)
 - Wang, Z.; Chen, J.; Hu, X.; *Thin Solid Films*, **2000**, 375, 238.
DOI: [10.1016/S0040-6090\(00\)01335-3](https://doi.org/10.1016/S0040-6090(00)01335-3)
 - Wang, Y.; Cao, G.; *Adv. Mater.*, **2008**, 20, 225.
DOI: [10.1002/adma.200702242](https://doi.org/10.1002/adma.200702242)
 - Liu, J.; Wang, X.; Peng, Q.; Li, Y.; *Adv. Mater.*, **2005**, 17, 764.
DOI: [10.1002/adma.200400993](https://doi.org/10.1002/adma.200400993)
 - Mai, L.; Xu, L.; Gao, Q.; Han, C.; Hu, B.; Pi, Y.; *Nano Letters*, **2010**, 10, 2604.
DOI: [10.1021/nl1013184](https://doi.org/10.1021/nl1013184)
 - Wang, Y.; Cao, G.; *Chem. Mater.*, **2006**, 18, 2787.
DOI: [10.1021/cm052765h](https://doi.org/10.1021/cm052765h)
 - Pawde, S.M.; Deshmukh, K.; *J. Appl Polym. Sci.*, **2006**, 101, 4167.
DOI: [10.1002/app.24079](https://doi.org/10.1002/app.24079)
 - Kim, H.; Baik, D.H.; Jeong, Y.G.; *Macromol. Res.*, **2012**, 20, 920.
DOI: [10.1007/s13233-012-0064-8](https://doi.org/10.1007/s13233-012-0064-8)
 - Zhang, H.; Wang, X.; Li, J.; Wang, F.; *Synth Met.*, **2009**, 159, 1508.
DOI: [10.1016/j.synthmet.2009.03.022](https://doi.org/10.1016/j.synthmet.2009.03.022)
 - Zhang, K.; Zhang, L.L.; Zhao, X.S.; Wu, J.; *Chem. Mater.*, **2010**, 22, 1392.
DOI: [10.1021/cm902876u](https://doi.org/10.1021/cm902876u)
 - Chiu, F.C.; Chen, C.C.; Chen, Y.J.; *J. Polym. Res.*, **2014**, 21, 378.
DOI: [10.1007/s10965-014-0378-7](https://doi.org/10.1007/s10965-014-0378-7)
 - Pawde, S.M.; Deshmukh, K.; *J. Appl. Polym. Sci.* **2008**, 110, 2569.
DOI: [10.1002/app.28761](https://doi.org/10.1002/app.28761)
 - Mohanapriya, M. K.; Deshmukh, K.; Ahamed, M.B.; Chidambaram, K.; Pasha, S.K.K.; *Mater. Today Proceed.*, **2016**, 3, 1864.
DOI: [10.1016/j.matpr.2016.04.086](https://doi.org/10.1016/j.matpr.2016.04.086)



Advanced Materials Letters

Volume 8, March 2017

Editor in Chief: Ashutosh Tiwari

An official journal of International Association of Advanced Materials

www.iaamonline.org

Available online at: www.vbripress.com


A Monthly Journal

Publish your article in this journal

Advanced Materials Letters is an official international journal of International Association of Advanced Materials (IAAM, www.iaamonline.org) published monthly by VBRI Press AB from Sweden. The journal is intended to provide high-quality peer-review articles in the fascinating field of materials science and technology particularly in the area of structure, synthesis and processing, characterisation, advanced-state properties and applications of materials. All published articles are indexed in various databases and are available download for free. The manuscript management system is completely electronic and has fast and fair peer-review process. The journal includes review article, research article, notes, letter to editor and short communications.

Copyright © 2017 VBRI Press AB, Sweden

www.vbripress.com/aml



VBRI Press
Commitment to Excellence